

provide a polar "barrier" to the approach of an alkyl side chain unit. The polymers are thus visualized as "comb-type" copolymers where the side chains are packed into the regions of space around the polymer backbone but do not penetrate or entangle with the backbone itself.

The behavior of ΔC_p^u and ΔC_p^L as functions of copolymer compositions can be gauged from the last two columns of Tables I-IV. A definite trend of increasing ΔC_p^u with increasing content of the shorter ester side chain is seen and such behavior is rationalized by the postulate that T_g^u originates primarily from main-chain relaxations. The relative number of main-chain units or segments is small in copolymers with a high, long-ester side-chain content but increases as the copolymer becomes richer in dimethyl or dipropyl itaconate units.

Tables I-IV also show that the ΔC_p^L values tend to decrease as the mole fractions of the longer side chains decrease, as would be expected if the relaxations involved are exclusive to these units. $\Delta C_p^{\text{tot}} = \Delta C_p^u + \Delta C_p^L$ should reflect the overall complexity of the repeat unit or number of "beads"⁸ and would be expected to decrease as the copolymers become richer in the comonomer of simpler structure. This is approximately so, but each copolymer series reaches a more or less constant ΔC_p^{tot} value at ca. 50% composition rather than at 100%. This behavior would seem rather unexpected, and it can only be suggested that the total amount of relaxation that is possible as the rubbery state is achieved occurs over a wider temperature range than encompassed by the two ΔC_p jumps and remains unquantified by $\Delta C_p^u + \Delta C_p^L$ as they are defined here.

Finally, it should be noted that the DSC-determined values of T_g^u and T_g^L quoted in this paper and derived

from C_p^{-T} curves differ considerably from those quoted earlier.² The samples used in this study and those used earlier have sufficiently large M_n values to ensure that T_g values have reached their asymptotic limit but will differ presumably to some extent in their distribution. This will account for a small part of the observed differences (which is up to 19 K in T_g^L for poly(di-*n*-decyl itaconate)) but not all. We have found that considerably different values for the onset of a T_g inflection can be inferred from data on the same polymer when it is displayed on a C_p^{-T} curve, as here, compared with the more common DSC trace, which is nonabsolute. This point is being investigated further, but we are of the opinion that the C_p measurements are the more reliable and the values obtained by this method will be more representative of the samples.

Registry No. Dimethyl itaconate-diheptyl itaconate copolymer, 65553-84-6; dimethyl itaconate-dioctyl itaconate copolymer, 78279-12-6; dipropyl itaconate-dioctyl itaconate copolymer, 85864-39-7; dimethyl itaconate-dinonyl itaconate copolymer, 85803-48-1.

References and Notes

- (1) Cowie, J. M. G.; Haq, Z.; McEwen, I. J. *J. Polym. Sci., Polym. Lett. Ed.* **1979**, *17*, 771.
- (2) Cowie, J. M. G.; Haq, Z.; McEwen, I. J.; Velickovic, J. *Polymer* **1981**, *22*, 327.
- (3) Cowie, J. M. G.; Ferguson, R.; McEwen, I. J. *Polymer* **1982**, *23*, 605.
- (4) Cowie, J. M. G.; McEwen, I. J.; Velickovic, J. *Polymer* **1975**, *16*, 869.
- (5) Cowie, J. M. G. *J. Macromol. Sci., Phys.* **1980**, *B18* (1), 569.
- (6) McEwen, I. J.; Lath, D., unpublished work.
- (7) Cowie, J. M. G.; Henshall, S. A. E.; McEwen, I. J.; Velickovic, J. *Polymer* **1977**, *18*, 613.
- (8) Wunderlich, B.; Baur, H. *Adv. Polym. Sci.* **1970/1971**, *7*, 151.

Theoretical Description of the Heat Capacity Change at the Lower Glass Transition Temperature of Poly(alkyl itaconates) Exhibiting Dual Glass Transition Behavior

John M. G. Cowie,* Roderick Ferguson, Iain J. McEwen, and Mehrdad Yazdani Pedram

Chemistry Department, University of Stirling,
Stirling FK9 4LA, Scotland, United Kingdom. Received December 6, 1982

ABSTRACT: The change in the heat capacity (ΔC_p^L) at the lower glass transition (T_g^L) in poly(di-*n*-alkyl itaconates) with 7-10 carbons in the side chain has been measured. A model for a side-chain relaxation mechanism is proposed that involves hindered rotation about C-C bonds, and the relevant partition function and heat capacity contribution from this motion has been evaluated. The calculated heat capacities have been compared with the experimental values in the region of T_g^L , and good agreement has been found.

Introduction

It has been demonstrated that the low-temperature inflections in the C_p - T curves described in the previous paper¹ and labeled T_g^L for the homopolymer series poly(di-*n*-heptyl itaconate) to poly(di-*n*-decyl itaconate) originate from independent motions of the side chains. In this paper we attempt a theoretical description of the heat capacity behavior at T_g^L based on a model of side-chain motion.

In the molten state the heat capacity of a high polymer is due to molecular vibrations and, in addition, conformational changes and internal rotations. When the liquid becomes a glass, large-scale molecular motion ceases and

the heat capacity is mainly accounted for by vibrational motion only. Smaller contributions that freeze out at $T < T_g$ come from limited internal rotations and movements of small groups of atoms or from changes between rotational isomers of differing energies. To our knowledge, only in the case of poly(dicyclooctyl itaconate) has it been possible to determine experimentally the heat capacity contribution from one such small-scale sub- T_g motion, and this was ascribed to changes of the cyclooctane ring between its nonequilibrium conformers.² In the present case the magnitude of the low-temperature inflection (ΔC_p^L) is very much larger, both relative to ΔC_p at the main-chain relaxation and in absolute terms, when com-

Table I
Frequencies of Infrared Vibrations per CH₂ Unit in the Spectra of Poly(di-*n*-alkyl itaconates)

vibration mode	frequency/cm ⁻¹
C-H stretch	2850
C-C stretch	950
C-H twist	1300
C-H wag	1300
C-H bend	1430
C-H rock	720

pared to that observed for poly(dicyclooctyl itaconate), and this implies that considerable molecular relaxation is occurring.

Experimental Section

Polymer characterization and differential scanning calorimetric determination of the heat capacity as a function of temperature for the samples is described in the preceding paper.¹

Discussion

In order to quantify the contribution from any particular molecular motion, one must know the heat capacity in the absence of that motion. Since each member of the di-*n*-alkyl itaconate series differs from the previous one by two CH₂ units, it should be possible to estimate the glassy-state C_p - T behavior of all the higher homologues from that of the first member (poly(dimethyl itaconate)) and to evaluate a contribution from

$$C_p(\text{CH}_2) \simeq C_v(\text{CH}_2) = \sum_i k \left(\frac{\Theta_i}{T} \right)^2 \frac{e^{\Theta_i/T}}{(e^{\Theta_i/T} - 1)^2} \quad (1)$$

where each CH₂ unit is considered to contribute i Einstein oscillators with characteristic frequencies $\Theta_i = h\nu_i/k$. k is the Boltzmann constant, h is Planck's constant, T is the temperature in kelvins, and ν_i is the frequency in s⁻¹ of the i th oscillator.

The frequencies are those of the normal modes of the added CH₂ unit and comprise two C-H stretching vibrations, four C-H bending type vibrations, one C-C stretching vibration, and two low-frequency ("acoustical") modes related to chain twisting and bending movements.³ All but the acoustical frequencies can be identified from the infrared spectra of the polymers, and these are listed in Table I. The remaining frequencies were chosen to obtain the best theoretical fits to the experimental heat capacities of the four homopolymers between 110 and 160 K using both eq 1 and eq 2, where T is in kelvins and C_p (PDMI) =

$$-60.412 + 1.9665T - 6.2194 \times 10^{-3}T^2 + 8.9016 \times 10^{-6}T^3 \quad (2)$$

is in J K⁻¹ (mol of repeat units)⁻¹. The latter equation represents the smoothed heat capacity of poly(dimethyl itaconate) between 110 and 270 K based on the data presented in the previous paper¹ and a least-squares curve fitting technique.

The values of the vibrational frequencies of the two acoustical modes used for each polymer are shown in Table II. These are almost identical for the first and the last members of the series but somewhat different for the other two. Nevertheless, the frequencies chosen are similar to those employed by Dole (320 and 90 cm⁻¹) to describe the acoustical components of the frequency spectrum used to calculate the C_p - T behavior of polyethylene.⁴

In the absence of any other molecular motions, eq 1 and 2 predict the subambient heat capacities of the poly(di-*n*-alkyl itaconates) to be smoothly increasing functions of temperature. In order to account for the occurrence of T_g^L ,

Table II
Frequencies of Acoustical Modes Used To Obtain Best Fits to Experimental Heat Capacities of Indicated Polymers between 110 and 160 K

polymer	frequencies/cm ⁻¹
poly(di- <i>n</i> -heptyl itaconate)	320, 50
poly(di- <i>n</i> -octyl itaconate)	200, 100
poly(di- <i>n</i> -nonyl itaconate)	290, 120
poly(di- <i>n</i> -decyl itaconate)	340, 40

which is believed to arise from independent side-chain relaxation, a model describing side-chain motion is presented in which the heat capacity change ΔC_p^L is due to hindered internal rotations about the C-C bonds of the side chain. By assuming the pertinent hindering potential, it is possible to calculate the heat capacity contribution due solely to hindered rotation.

Calculation of Hindered Rotation Heat Capacity. This is related to the partition function Q for the system by

$$C_p \simeq C_v = \frac{R}{T^2} \frac{\partial^2 \ln Q}{\partial (1/T)^2} \quad (3)$$

In the present case the difference between C_p and C_v is neglected. Furthermore

$$C_v = R(Q_0 Q_2 - Q_1^2)/Q_0^2 \quad (4)$$

where $Q_0 = Q = \sum_i g_i e^{-(w_i/kT)} = \sum_i g_i e^{-U_i}$, $Q_1 = \sum_i g_i U_i e^{-U_i}$, $Q_2 = \sum_i g_i U_i^2 e^{-U_i}$, and g_i is the degeneracy of the i th energy level w_i .

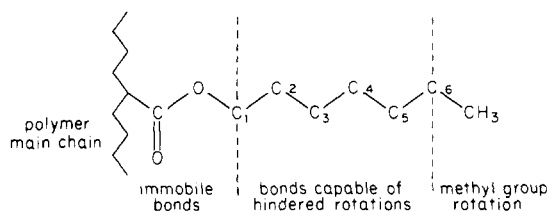
Pitzer⁵ has shown that the contribution to the heat capacity from all hindered internal rotations in an *n*-alkane can be written as

$$C_v = (n - 3)C_v^{i, \text{rot}} + C_v^{\text{steric}} \quad (5)$$

Here, n is the number of carbon atoms in the chain, and $C_v^{i, \text{rot}}$ is the contribution to the heat capacity from ethane-like internal rotations. C_v^{steric} is the contribution arising from steric interactions of the chain with itself, involving other than trans configurations. $C_v^{i, \text{rot}}$ is identical with the function " C " tabulated by Pitzer,^{5,6} although it proved necessary to calculate values outside the range published.⁷ Solution of the appropriate wave equation yields the values of $w_i^{i, \text{rot}}$ for use in eq 4.

C_v^{steric} was calculated by Pitzer's method,⁶ where again the published table giving the number of configurations (g_i) with a given steric energy $w_i^{\text{steric}} = ja$ was extended to cover *n*-alkanes up to C₁₀. j is a positive integer and a is an energy chosen by comparison with the measured heat capacities of gaseous *n*-alkanes. A schematic of the potential diagram used to describe one hindered rotation is shown in Figure 1. All calculations were carried out on a VAX 11/780 computer, and the results are shown in Figure 2.

Hindered Internal Rotation Model. The following model for motion in an *n*-alkyl side chain is proposed and illustrated below for poly(di-*n*-heptyl itaconate).



Space-filling CPK molecular models show that rotation about both the main-chain carbon-carbonyl carbon bond

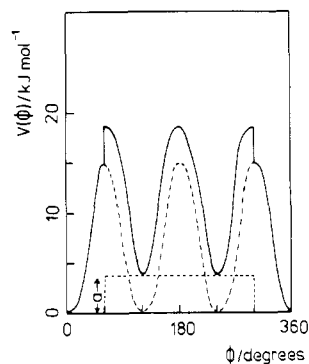


Figure 1. Potential diagram for one hindered rotation in an *n*-alkyl chain (—), $V(\phi) = (V_0/2)[1 - \cos(3\phi)] + V_1$. $V_1 = a$ for $60^\circ < \phi < 300^\circ$ but zero otherwise, $V_0 = 15.06 \text{ kJ mol}^{-1}$, and $a = 3.8 \text{ kJ mol}^{-1}$.

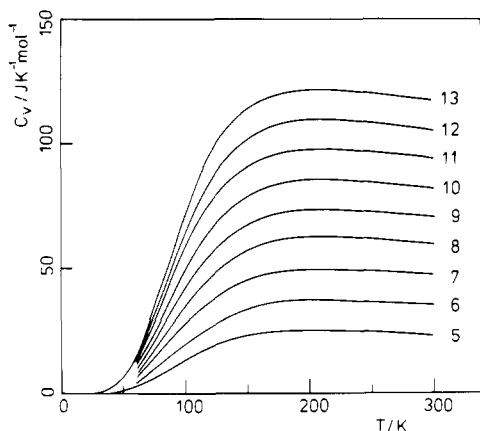


Figure 2. Contributions to the heat capacity C_v from hindered rotation in *n*-alkanes as a function of temperature. The number of carbon atoms per alkane is indicated on the figure.

and the carbonyl carbon-ester oxygen bond is highly restricted and both are thus considered "locked" in the temperature range of interest. The potential barrier to rotation about the ester oxygen- C_1 bond has been calculated⁷ as $\sim 200 \text{ kJ mol}^{-1}$ and is considered to be effectively locked for the purposes of this model. Rotation of the end methyl group is known to occur in the temperature range $75\text{--}90 \text{ K}$ ⁸ and this contribution to the heat capacity will be accounted for in the C_p - T behavior of poly(dimethyl itaconate).

The remaining five rotations involving carbons 1-6 are considered to be the basis of the molecular motion contributing to the increase in heat capacity at T_g^L , and this is quantified by twice the hindered internal rotational heat capacity of *n*-octane. Similarly, *n*-nonane, *n*-decane, and *n*-undecane are used as models for calculating ΔC_p^L values for poly(di-*n*-octyl itaconate), poly(di-*n*-nonyl itaconate), and poly(di-*n*-decyl itaconate), respectively.

A further assumption is now made that below a certain temperature all internal side-chain rotation is completely frozen, but above this temperature rotation is allowed. The temperature defining the onset of motion is indicated by the position of the T_g^L damping peak obtained from the TBA thermograms of the long side chain *n*-alkyl itaconate polymers.^{1,9} These, of course, cover considerable temperature ranges over which an increasing number of side chains begin to relax, and the choice of a single temperature of 210 K is arbitrary. Below 210 K no contribution to the theoretical heat capacity (defined by eq 1 and 2) is obtained from hindered rotation, whereas above 210 K all the relevant internal rotations are considered to contribute amounts calculated from eq 4 and 5.

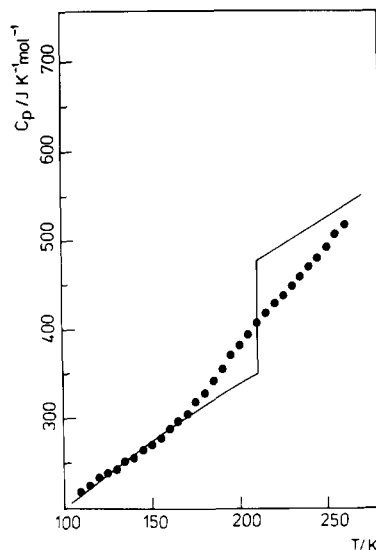


Figure 3. Experimental heat capacity per mole of repeat units for poly(di-*n*-heptyl itaconate) (●) and theoretical heat capacity (—) calculated as described in the text.

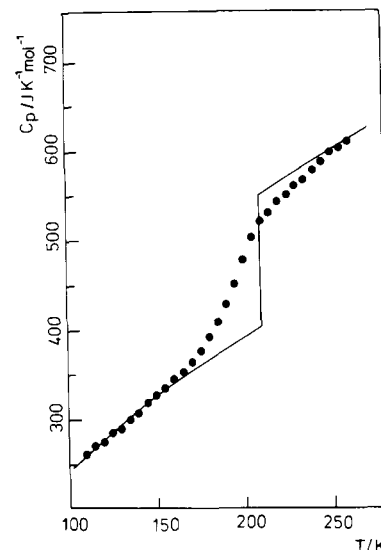


Figure 4. Experimental heat capacity per mole of repeat units for poly(di-*n*-octyl itaconate) (●) and theoretical heat capacity (—) calculated as described in the text.

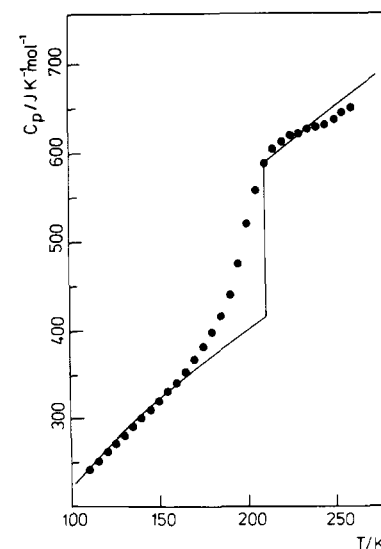


Figure 5. Experimental heat capacity per mole of repeat units for poly(di-*n*-nonyl itaconate) (●) and theoretical heat capacity (—) calculated as described in the text.

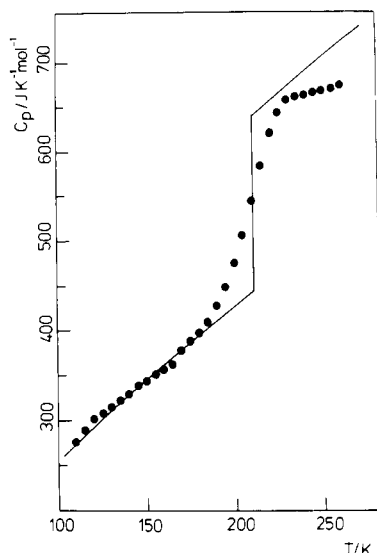


Figure 6. Experimental heat capacity per mole of repeat units for poly(di-*n*-decyl itaconate) (●) and theoretical heat capacity (—) calculated as described in the text.

Conclusions from the Internal Rotation Model. The experimental heat capacities for the four polymers are plotted from 110 to 260 K in Figures 3–6. Above 260 K the influence of T_g^u is apparent, introducing a second discontinuity in the C_p - T curve. Between 100 and 210 K the theoretical heat capacities, based on eq 1 and 2 and fitted as described earlier, are shown as solid lines, and at 210 K the contribution from the appropriate number of hindered rotations is added to give the total heat capacity of the systems due to vibrational sources and side-chain motion.

The agreement between the experimental heat capacity changes at T_g^L and those calculated from the proposed model is remarkably good considering the assumptions that are involved, for example, the application of isolated-molecule parameters to the situation pertaining in a condensed phase. Apart from poly(di-*n*-heptyl itaconate), the predicted heat capacity at $T > T_g^L$ is also quite satisfactory, although it should be remembered that this depends also on the extrapolated C_p - T behavior, evaluated from eq 1 and 2, remaining a reliable guide to "base line" behavior over almost 200 K. Nevertheless, it is felt that the concordance of experiment and the present theory shown in Figures 3–6 reinforces the proposal that the origin of T_g^L is independent movement of the side chain, which is effectively decoupled from any main-chain motion. Since the partition function used in the calculation is one that quantifies the heat capacity contribution from the chosen number of hindered rotations about C–C bonds, it is implicit in the thermodynamic argument that all possible

rotations are being performed simultaneously. The application of the model thus implies that T_g^L results from a cooperative-type movement of the whole side chain and not from a localized motion of a few units such as at T_g^1 .

Further evidence for a cooperative motion may be obtained from a consideration of the apparent activation energies (ΔH^*) at T_g^L , which have been measured for poly(di-*n*-heptyl itaconate), poly(di-*n*-octyl itaconate), and poly(di-*n*-nonyl itaconate) as approximately 230, 170, and 150 kJ mol⁻¹, respectively.⁹ Whereas the activation energies of localized molecular relaxations in polymer glasses fit the Heijboer relationship^{2,10}

$$\Delta H^*/\text{kJ mol}^{-1} = A(T_m/K) \quad (6)$$

(where ΔH^* is defined by the local barrier to movement, and T_m is the temperature of the 1-Hz damping maximum for the motion with A a constant ≈ 0.25), the values above do not, and consequently it is unlikely that they originate from small-scale motions involving only a limited number of atoms. T_g^L thus has most of the characteristics of a "conventional" glass transition rather than those of a sub-glass transition.

A final comment on the hindered rotation model can be made with regard to C_v^{steric} . The heat capacity from this source is evaluated on the basis of an all-trans ground state, and thus we are assuming that the side chains are capable of adopting such a conformation as the T_g^L motion is frozen in on cooling. If other conformations are frozen in, the contribution to C_v^{steric} at 210 K will be reduced proportionally and, since the ratio $C_v^{\text{steric}}/(C_v^{\text{steric}} + C_v^{\text{i,rot}})$ varies from ~ 0.38 to ~ 0.29 in the temperature range of interest, some error in the total contribution will result. On the basis of the known facility with which polymethylene sequences attain an all-trans state prior to crystallization, it is thought that any error from this source will be considerably less than that indicated by the values above.

Registry No. Poly(diheptyl itaconate), 28451-56-1; poly(dioctyl itaconate), 28451-57-2; poly(dinonyl itaconate), 28451-58-3; poly(didecyl itaconate), 28451-59-4.

References and Notes

- (1) Cowie, J. M. G.; McEwen, I. J.; Yazdani Pedram, M. *Macromolecules*, preceding paper in this issue.
- (2) Cowie, J. M. G.; Ferguson, R.; McEwen, I. J. *Polymer* **1982**, *23*, 605.
- (3) Wunderlich, B.; Baur, H. *Adv. Polym. Sci.* **1970/1971**, *7*, 151.
- (4) Dole, M. *Fortschr. Hochpolym.-Forsch.* **1960**, *2*, 221.
- (5) Pitzer, K. S. *J. Chem. Phys.* **1940**, *8*, 711.
- (6) Pitzer, K. S.; Gwinn, W. D. *J. Chem. Phys.* **1942**, *10*, 428.
- (7) Cowie, J. M. G.; Ferguson, R., unpublished work. Details of the calculation and Pitzer's extended table are available.
- (8) Cowie, J. M. G. *J. Macromol. Sci., Phys.* **1980**, *B18* (4), 569.
- (9) Cowie, J. M. G.; Haq, Z.; McEwen, I. J.; Velickovic, J. *Polymer* **1981**, *22*, 327.
- (10) Heijboer, J. *Ann. N.Y. Acad. Sci.* **1976**, *279*, 104.